Application of the extended P+QQ force model to $N \approx Z$ fp shell nuclei

M. Hasegawa [a], K. Kaneko [b] and S. Tazaki [c]

[a] *Laboratory of Physics, Fukuoka Dental College, Fukuoka 814-0193, Japan*

[b] *Department of Physics, Kyushu Sangyo University, Fukuoka 813-8503, Japan*

[c] *Department of Applied Physics, Fukuoka University, Fukuoka 814-0180, Japan*

Abstract

To study collective motion, the extended pairing plus QQ force model proposed recently is applied to A=46, 48 and 50 nuclei in the fp shell region. Exact shell model calculations in the truncated model space $(f_{7/2}, p_{3/2}, p_{1/2})$ prove the usefulness of the interaction. The simple model with the pairing plus quadrupole pairing plus QQ force and J-independent isoscalar proton-neutron force reproduces unexpectedly well observed binding energies, energy levels of collective (yrast) states and reduced $E2$ transition probabilities in ^{46}Ti, ^{46}V, ^{48}V, ^{48}Cr, ^{50}Cr and ^{50}Mn. The correspondence between theory and experiment is almost comparable to that attained by the full fp shell model calculations with realistic effective interactions. Some predictions are made for energy levels and variations of $B(E2)$ in the yrast bands, in these nuclei. Characteristics of the interaction are investigated by comparing with the realistic effective interactions.

PACS: 21.60.-n;21.10.Dr;21.10.Hw;21.10.Re

Key words: extended pairing plus quadrupole force; p-n interactions; shell model calculation; A=46, 48, 50 nuclei; ground-state energies; energy levels; B(E2).

1 Introduction

Two approaches starting from different pictures are crossing in fpg shell region: one is in progress along the pairing plus quadrupole $(P_0 + QQ)$ force model [1–6] and the other is the shell model approach using various effective interactions [7–15]. With the advancement of computer, the shell model approach has been extending the scale of calculation and the sphere of study [16–23]. The full fp shell model calculations with the KB3 interaction [16,21–23] have successfully explained the microscopic structure of the $f_{7/2}$ shell nuclei,

and are pushing the front of study to $A \approx 52$. On the other hand, the P_0+QQ force written in the isospin invariant form seems to qualitatively explain some properties of nuclei in the fp shell region [24–26]. One could expect a relationship between the two approaches and between the two types of interactions. In fact, it was shown [27] that an important part of the realistic interactions is approximated by the P_0+QQ force. The P_0+QQ force accompanied by the quadrupole pairing (P_2) force has succeeded in explaining the backbending mechanism of ^{48}Cr [28]. We note here that including both of $T=0$ and $T=1$ proton-neutron (p-n) interactions in the P_0+QQ force is recommended [25].

In a recent paper [29], we have shown that the P_0+QQ force can be extended so as to get near to realistic effective interactions. The extended interaction is composed of the four typical forms of interactions, i.e., the isospin invariant P_0+P_2+QQ force and J-independent isoscalar p-n force ($V_{\pi\nu}^{\tau=0}$). This form very harmonizes with the design of Ref. [27]. The calculations [29,30] showed that the isoscalar p-n force $V_{\pi\nu}^{\tau=0}$ plays a decisive role in reproducing the gross nuclear properties such as the binding energy, symmetry energy, etc., and that the $P_0+P_2+QQ+V_{\pi\nu}^{\tau=0}$ interaction describes considerably well the $f_{7/2}$ and $g_{9/2}$ shell nuclei in which a subshell dominates. The usefulness of the model, however, was studied within the single j shell model calculations there. The P_0+QQ force model originally aims to describe nuclear collective motion. The next crucial step is, therefore, to examine whether the extended P_0+QQ force model is quantitatively applicable to real situations having many j shells and is capable of describing the collective motion or not. This examination will show to what extent the picture of the P_0+QQ force model persists by a modification in various regions. We have confirmed that our interaction can describe the global features of p-n interactions and symmetry energy in another paper [31]. The purpose of this paper is to investigate in detail the applicability of the $P_0+P_2+QQ+V_{\pi\nu}^{\tau=0}$ interaction model by a realistic treatment of the $f_{7/2}$ shell nuclei.

We carry out exact shell model calculations in even-A nuclei with $A=44-50$ in order to see products of the interaction without any disturbance due to approximate treatment. This makes it easy to compare our interaction with the realistic effective interactions. We must determine the four force strengths when dealing with the $P_0+P_2+QQ+V_{\pi\nu}^{\tau=0}$ interaction. Unfortunately, the authors do not have a fast computer code enough for searching appropriate force strengths in the full fp shell. We therefore adopt the configuration space ($f_{7/2}$, $p_{3/2}$, $p_{1/2}$) as a model space. Calculations prove the usefulness of this model space especially for our interaction including the $V_{\pi\nu}^{\tau=0}$ force (the reason will be explained in Sec. IV). Our simple model with only four force strengths in the small configuration space gives unexpectedly good results in A=46, 48 and 50 nuclei with $N \approx Z$, which almost match the full fp shell model calculations with the KB3 interaction [16,21–23], so that we can discuss properties of these nuclei in our model and give information unreported previously.

This paper is organized as follows. In Sec. II, we briefly review the model. The results of calculations on the binding energies, energy levels and electric transition probabilities $B(E2)$ are shown for ^{46}Ti, ^{46}V, ^{48}V, ^{48}Cr, ^{50}Cr and ^{50}Mn in Sec. III. The dependence of the results on the model, the relation of our interaction to the realistic effective interactions and properties of the collective yrast bands are discussed in Sec. IV. Concluding remarks are given in Sec. V.

2 The model

We have proposed the following isospin-invariant Hamiltonian composed of the four forces, P_0, P_2, QQ and $V_{\pi\nu}^{\tau=0}$, and have discussed the basic properties of it in Ref. [29]:

$$H = H_{\rm sp} + V(P_0) + V(P_2) + V(QQ) + V_{\pi\nu}^{\tau=0}, \tag{1}$$

$$H_{\rm sp} = \sum_a \epsilon_a(\hat{n}_{a\pi} + \hat{n}_{a\nu}), \tag{2}$$

$$V(P_J) = -\frac{1}{2} g_J \sum_{M\kappa} \sum_{a\le b} \sum_{c\le d} p_J(ab) p_J(cd) A^\dagger_{JM1\kappa}(ab) A_{JM1\kappa}(cd), \tag{3}$$

$$V(QQ) = -\frac{1}{2}\chi' \sum_M \sum_{ac\rho} \sum_{bd\rho'} q'(ac) q'(bd) : B^\dagger_{2M\rho}(ac) B_{2M\rho'}(bd) : \tag{4}$$

$$V_{\pi\nu}^{\tau=0} = -k^0 \sum_{a\le b} \sum_{JM} A^\dagger_{JM00}(ab) A_{JM00}(ab), \tag{5}$$

with

$$A^\dagger_{JM\tau\kappa}(ab) = [c^\dagger_a c^\dagger_b]_{JM\tau\kappa}/\sqrt{1+\delta_{ab}}, \quad B^\dagger_{JM\rho}(ac) = [c^\dagger_{a\rho} c_{c\rho}]_{JM}, \tag{6}$$

$$p_0(ab) = \sqrt{2j_a+1}\delta_{ab}, \quad p_2(ac) = q'(ac) = (a\|r^2 Y_2/b_0^2\|c)/\sqrt{5}. \tag{7}$$

Here $\hat{n}_{a\pi}$ and $\hat{n}_{a\nu}$ are the proton- and neutron-number operators for a single-particle orbit a, the symbol : : in $V(QQ)$ means the normal order product of four nucleon operators, ρ denotes the z-components of isospin $\pm\frac{1}{2}$ and b_0 is the harmonic-oscillator range parameter. This Hamiltonian has only the four force parameters, g_0, g_2, χ', and k^0, in addition to the single-particle energies ϵ_a. We call the $P_0 + P_2 + QQ + V_{\pi\nu}^{\tau=0}$ interaction "functional effective interaction (FEI)" in this paper.

As shown in Ref. [29], the J-independent isoscalar p-n force $V_{\pi\nu}^{\tau=0}$ is reduced to

$$V_{\pi\nu}^{\tau=0} = -\frac{1}{2}k^0\{\frac{\hat{n}}{2}(\frac{\hat{n}}{2}+1) - \hat{T}^2\}, \tag{8}$$

where the operator $\hat{n}$ stands for the total number of the valence nucleons and $\hat{T}$ for the total isospin, i.e., $\hat{n} = \hat{n}_p + \hat{n}_n = \sum_a (\hat{n}_{a\pi} + \hat{n}_{a\nu})$ and $\hat{T} = \sum_a \hat{T}_a$. For the states with the isospin $T = (n_n - n_p)/2$, this force can be rewritten as

$$\langle V_{\pi\nu}^{\tau=0} \rangle = -\frac{1}{2} k^0 n_p (n_n + 1). \tag{9}$$

In our isospin invariant Hamiltonian, two conjugate nuclei with $T = (n_n - n_p)/2 = (n_p - n_n)/2$ are equivalent to each other, and the $T = 1$ states in odd-odd nuclei with $N = Z = A/2$ are equivalent to those in even-even nuclei with $Z = A/2 - 1$ and $N = A/2 + 1$. The p-n force $V_{\pi\nu}^{\tau=0}$ is indispensable for the binding energy but does not change the wave functions determined by the $P_0 + P_2 + QQ$ force. The $V_{\pi\nu}^{\tau=0}$ force is the main origin of the symmetry energy [30] and brings a shift to the energy space between the states with different isospins in a nucleus. The shell model Hamiltonian is originated in the Hartree-Fock (HF) picture and the single-particle energies ϵ_a stand for the single-particle mean field determined by the HF theory. The p-n force $V_{\pi\nu}^{\tau=0}$ in the simple expression (9) suggests that $V_{\pi\nu}^{\tau=0}$ is probably related to the HF variation and may be an average term by which the mean field is accompanied. If we extract $V_{\pi\nu}^{\tau=0}$, residual interaction in the mean field comes from the P_0, P_2 and QQ forces in our model. This interpretation is similar to that of Dufour and Zuker [27]. The residual $P_0 + P_2 + QQ$ interaction can be understood based on the Bohr-Mottelson picture [4]. This problem how to explain the phenomenologically introduced p-n force $V_{\pi\nu}^{\tau=0}$ should be discussed further.

The Hamiltonian (1-5) describes the energy of valence nucleons outside the doubly-closed-shell core (^{40}Ca) excluding the Coulomb energy. The corresponding experimental energy is evaluated as

$$W_0(Z, N) = B(Z, N) - B(^{40}\mathrm{Ca}) - \lambda(A - 40) - \Delta E_{\mathrm{C}}(n_p, n_n), \tag{10}$$

where $B(Z, N)$ is the nuclear binding energy and λ is the base level of single-particle energies. We fix $\lambda = -8.364$ MeV so that $W_0(^{41}\mathrm{Ca}) = W_0(^{40}\mathrm{Ca}) = 0.0$ and the lowest single-particle energy $\epsilon_{7/2}$ becomes zero, and evaluate the Coulomb energy correction $\Delta E_{\mathrm{C}}(n_p, n_n)$ by the function [32]

$$\Delta E_{\mathrm{C}}(n_p, n_n) = 7.279\, n_p + 0.15\, n_p(n_p - 1) - 0.065\, n_p n_n. \tag{11}$$

We shall compare calculated ground-state energies with the experimental energies $W_0(Z, N)$.

We adopt the model space $(f_{7/2}, p_{3/2}, p_{1/2})$ as mentioned in Introduction. Results of calculations depend on the single-particle energies ϵ_a and the four force

parameters g_0, g_2, χ' and k^0. We take ϵ_a from the experimental spectrum of ^{41}Ca (we fix $\epsilon_{7/2} = 0$ mentioned above) as follows:

$$\epsilon_{7/2} = 0.0, \quad \epsilon_{3/2} = 1.94, \quad \epsilon_{1/2} = 3.61 \quad \text{in MeV.} \tag{12}$$

We employed fixed numbers for g_0, g_2 and χ' in the single j model in Refs. [29,30]. Calculations, however, recommend using A-dependent parameters for the P_0, P_2 and QQ forces in the present many j shell case as the ordinary treatment of these forces. We put the same $1/A$ dependence on k^0 as in Refs. [29,30]. A rough parameter search in $A = 46 - 50$ nuclei leads us to the values

$$\begin{aligned} &g_0 = 0.48(42/A), \quad g_2 = 0.36(42/A)^{5/3}, \\ &\chi' = 0.30(42/A)^{5/3}, \quad k^0 = 2.23(42/A), \quad \text{in MeV.} \end{aligned} \tag{13}$$

We do not readjust the seven parameters in each nucleus.

The present calculations are considerably realistic and are expected to provide good information about wave functions. To test the wave functions, we calculate the reduced quadrupole transition probabilities $B(E2)$ and compare them with observed values. Following Caurier *et al.* [16], we also calculate the intrinsic quadrupole moment Q_0 by the equations

$$Q_0 = \frac{(J+1)(2J+3)}{3K^2 - J(J+1)} Q_{spec}(J) \quad \text{for } K \neq 1, \tag{14}$$

$$B(E2 : J_i \to J_f) = \frac{5}{16\pi} e^2 \langle J_i K 20 | J_f K \rangle^2 Q_0^2, \tag{15}$$

where $Q_{spec}(J)$ is the spectroscopic quadrupole moment $\sqrt{16\pi/5}\langle JJ|Q^\dagger_{20}|JJ\rangle$ with $Q^\dagger_{2M\rho} = e_\rho b_0^2 \sum_{ac} q'(ac)[c^\dagger_{a\rho} c_{c\rho}]_{2M}$ and K is the projection of the total spin on the intrinsic axis. We use the harmonic-oscillator range parameter $b_0 = 1.01A^{1/6}$ fm, and effective charges of $1.5e$ for protons and $0.5e$ for neutrons in the calculations of $B(E2)$ and Q_0. These values are the same as those used in Refs. [16,19,21–23]. We denote the intrinsic quadrupole moment calculated from Eq. (14) by $Q_0^{(s)}$ and that calculated from Eq. (15) by $Q_0^{(t)}$ following Martínez-Pinedo *et al.* [22].

3 The results of calculations

We have carried out exact shell model calculations with the model shown in Sec. II in A=46, 48 and 50 systems. The ground-state energies obtained are listed in Table 1, where the experimental energies W_0 are calculated

from mass excesses [33] using Eqs. (10) and (11). Our simple interaction $P_0+P_2+QQ+V_{\pi\nu}^{\tau=0}$ reproduces the experimental energies well. The agreement is excellent for the $N = Z$ nuclei, ^{46}V, ^{48}Cr and ^{50}Mn. Note that our model systematically reproduces the energies of different-number nuclei within a single set of parameters. The results confirm the essential role of the J-independent isoscalar p-n force $V_{\pi\nu}^{\tau=0}$ in the binding energies of $N \approx Z$ nuclei which is stressed in our previous papers [29,30]. It is certain that an important part of nucleon-nucleon interactions can be written as $V_{\pi\nu}^{\tau=0}$.

Table 1
Ground-state energies of $A = 46, 48, 50$ nuclei.

	^{46}Ti(^{46}V,0$^+$)	^{48}Ti	^{48}V(4$^+$)	^{48}Cr	^{50}V(6$^+$)	^{50}Cr(^{50}Mn,0$^+$)
W_0	-20.28	-23.82	-26.71	-32.38	-30.48	-38.71
Calc.	-20.17	-23.44	-26.79	-32.38	-30.00	-38.72

The $P_0 + P_2 + QQ + V_{\pi\nu}^{\tau=0}$ interaction, however, cannot give enough binding energies as N separates from Z. Especially, the disagreement becomes large when the number of valence protons or neutrons is 0 and 1. This is in contrast to that the KB3 interaction overbinds the A=48 nuclei about 0.78 MeV but provides very good relative binding energies of all the A=48 nuclei [16]. We shall discuss the difference of our interaction from the realistic interactions in the next section.

In the following subsections, we show calculated excitation energies and electric quadrupole properties in ^{46}Ti, ^{46}V, ^{48}V, ^{48}Cr, ^{50}Cr and ^{50}Mn with $Z, N \geq 42$ where the $P_0 + P_2 + QQ + V_{\pi\nu}^{\tau=0}$ interaction works well. Only positive-parity states are considered in our model space. It should be remembered here that the energy spectra and wave functions are determined by the $P_0 + P_2 + QQ$ force in our model, and the $V_{\pi\nu}^{\tau=0}$ force causes only an energy shift depending on the valence nucleon number and isospin.

3.1 ^{46}*Ti*

Calculated excitation energies and $E2$ transition probabilities in ^{46}Ti are compared with observed ones [33–35] in Fig. 1 and Table 2. The yrast levels (the lowest-energy state of each spin) are satisfactorily reproduced in spite of the simple model. We can regard the 0_1^+, 2_1^+, 4_1^+ ... 14_1^+ states as the ground-state band. They are connected by the large $E2$ transition probabilities, especially up to the 10_1^+ state. The observed $B(E2 : J \to J-2)$ values in the ground-state band are considerably well reproduced by our model though the model space does not include the $f_{5/2}$ orbit. The spectroscopic quadrupole moments (Q_{spec}) of the 0_1^+, 2_1^+..... 14_1^+ states have a minus sign and their values are in the range 19-26 e fm^2. The intrinsic quadrupole moments $Q_0^{(s)}$ and $Q_0^{(t)}$

are large and roughly constant up to the 10^+_1 state, which tells us that these states are collective and have the same nature. The observed energy levels of the ground-state band show the backbending at the 10^+_1 state. The calculated energy levels also show a similar tendency, though the position of the 10^+_1 state is not very good. The calculated intrinsic quadrupole moment $Q_0^{(t)}$ suggests different structure at least above the 10^+_1 state.

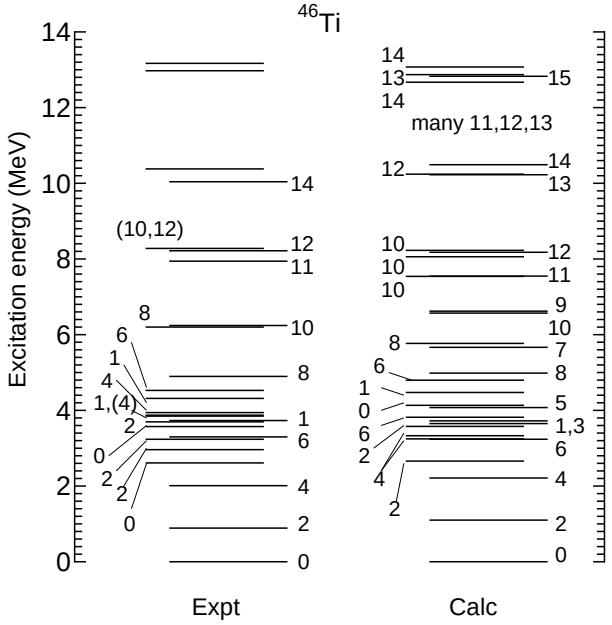

Fig. 1. Calculated and observed energy levels of ^{46}Ti.

From the good reproduction of the 1^+_1 and 11^+_1 levels as well as the ground-state band, the calculated energy levels of the J=odd yrast states probably provide a good prediction for their positions. This will be tested in future experiments.

In Fig. 1, we also compare calculated low energy levels below 4 MeV and a couple of levels above it with observed ones, where we omit 4 levels assigned as $J^\pi = 2^+$ and 7 other levels with indefinite spin and parity [33] from the experimental column in order to avoid overcrowding. We can suppose that some of the observed states including the 0^+_2 state at 2.661 MeV are core-excited states (probably 8-particle-2-hole ones) on the analogy of the core-excited states in ^{44}Ti. The calculated energy levels of non-collective states lie at a good position roughly speaking and the level density looks good if we exclude the core-excited states.

The state at 10.040 MeV, which was assigned as J=12 before [36], was recently identified as J=14 [35], because the transition to 11^+_1 was not detected. The calculated $B(E2)$ values, $B(E2:14_1 \to 12_1)$=26, $B(E2:12_2 \to 12_1)$=3.3 and $B(E2:13_1 \to 12_1)$=0.1 in e^2 fm^4, suggest that the two levels at 10.040 MeV and 10.380 MeV are probably 14^+_1 and 12^+_2, though their order is inverse in

our prediction. The present calculation also provides candidates for the two observed levels at 12.974 MeV and 13.169 MeV. They are possibly the 14_2^+ and 15_1^+ states from the calculated $B(E2)$ values.

Table 2
Electric quadrupole properties of the yrast and other states in ^{46}Ti. The observed $B(E2)$ values are taken from Refs. [30] (Expt.1) and [31] (Expt.2).

$J_n \to J'_m$	$B(E2: J_n - J'_m)$ in e^2 fm^4			calculated Q_{spec}, Q_0 in e fm^2		
	Expt.1	Expt.2	Calc.	$Q_{spec}(J_n)$	$Q_0^{(s)}$	$Q_0^{(t)}$
$2_1 \to 0_1$	197±32		119	-18.9	66	77
$4_1 \to 2_1$	192±32		159	-24.5	67	75
$6_1 \to 4_1$	158±28		141	-21.3	53	67
$8_1 \to 6_1$	119±38,	62±30	126	-23.7	56	62
$8_2 \to 6_1$			0.03	-11.1	27	
$\to 8_1$			8.8			
$10_1 \to 8_1$	152±15,	77±36	104	-26.3	61	56
$10_2 \to 10_1$			3.8	-12.1	28	
$\to 8_1$			3.7			
$\to 8_2$			46			
$12_1 \to 10_1$	25±10,	22±7	53	-22.3	50	39
$12_2 \to 10_1$			17	-18.9	43	
$\to 11_1$			7.8			
$\to 12_1$			3.3			
$\to 10_2$			0.3			
$13_1 \to 12_1$			0.1			
$14_1 \to 12_1$	46±30,	>44	26	-22.8	51	27
$\to 13_1$			9.5			
$15_1 \to 14_1$			2.6			
$\to 14_2$			3.0			
$14_2 \to 14_1$			6.2	-23.1	51	
$\to 12_2$			12			

3.2 ^{46}V

Recently, the $N = Z$ odd-odd nucleus $^{46}_{23}V_{23}$ has been studied by elaborate experiments [37,38]. Let us compare calculated energy levels of the $T = 0$ yrast states with observed ones in Fig. 2. Our interaction somewhat overbinds the $T = 0$ low-spin states as the realistic effective interactions do [37,38]. It is still notable that such a simple force $V_{\pi\nu}^{\tau=0}$ improves so well both the binding energy and relative energy between the $T = 0$ and $T = 1$ states. If we regard the $T = 0$ yrast states 3_1^+, 4_1^+, 5_1^+ ... 15_1^+ as a collective band based on the 3_1^+ state, the theoretical pattern of excitation is very similar to the observed pattern. The order of spin in the band is correctly reproduced. The correspondence of the excitation energies measured from the 3_1^+ level between theory and experiment is good.

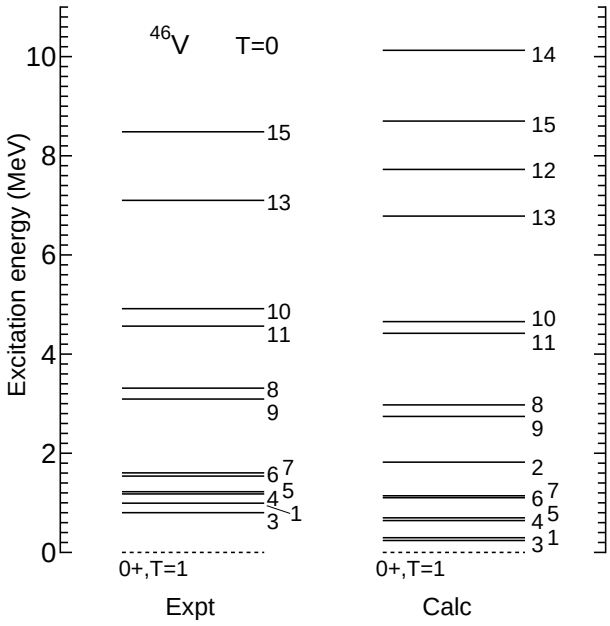

Fig. 2. Calculated and observed energy levels of ^{46}V. Only the yrast states with $T = 0$ are shown.

The calculated $B(E2)$ values listed in Table 3 support that the yrast states 3_1^+, 4_1^+, 5_1^+, 6_1^+ and 7_1^+ in order of spin J are members of a collective band, because they are connected by large $B(E2 : J \to J-1)$. The spectroscopic quadrupole moment Q_{spec} shows a rapid change as J increases till 8_1^+ , and then becomes nearly constant (-20 to -25 e fm^2). Above 7_1^+, the pair states with even spin $2J$ and odd spin $2J+1$ reverse their order in energy and the two series of states with odd J and even J connected by large $B(E2 : J \to J-2)$ stand out. We can guess a structure change in the band between 7_1^+ and 9_1^+. Is it possible to regard the two series, 9_1^+, 11_1^+ .... 15_1^+ and 8_1^+, 10_1^+ ....14_1^+, as two quasi-bands? The γ transitions observed in Ref. [38] seem to display this feature.

Table 3
Calculated $B(E2)$ (in e^2 fm^4) and Q_{spec} (in e fm^2) with respect to the $T = 0$ yrast states in ^{46}V.

$J \to J'$	$B(E2)$	Q_{spec}	$J \to J'$	$B(E2)$	Q_{spec}
3		33.2	$10 \to 8$	91	-25.2
$4 \to 3$	249	12.0	$\to 9$	24	
$5 \to 3$	60	-4.1	$\to 11$	31	
$\to 4$	207		$11 \to 9$	129	-21.9
$6 \to 4$	85	-10.6	$12 \to 10$	71	-21.2
$\to 5$	165		$\to 11$	7.2	
$7 \to 5$	46	-14.8	$\to 13$	22	
$\to 6$	122		$13 \to 11$	99	-23.3
$8 \to 6$	111	-21.5	$14 \to 12$	33	-24.0
$\to 7$	68		$\to 13$	7.6	
$9 \to 7$	142	-20.3	$\to 15$	44	
$8 \to 9$	75		$15 \to 13$	65	-22.0

In Ref. [37], the low-lying states of ^{46}V were examined by the full fp shell model calculations with the realistic effective interactions, KB3 [16] and FPD6 [14]. We compare the result obtained using our interaction FEI with the results of Ref. [37], in Fig. 3. In this figure, all the energy levels below 3.25 MeV including unknown-parity levels but excluding the negative-parity ones are shown (6_1^+ and 4_2^+ with $T = 1$ are added). The calculated $T = 0$ levels are shifted so that 3_1^+ is situated at the observed position 0.801 MeV as done in Ref. [37]. The shift 0.56 MeV for the FEI is a little larger than 0.436 MeV for the KB3 and 0.498 MeV for the FPD6. For the $T = 0$ states, the FEI result seems to be better than the FPD6 one and considerably match the KB3 one. The FEI result for the $T = 1$ levels is not very bad as compared with the KB3 and FPD6 results. The non-collective states except the yrast states obtained by the FEI have a tendency to go down (this tendency is observed in other systems). The number of the energy levels obtained by the FEI may be too many below 3.25 MeV but is smaller than that of the observed levels. The levels shown in the column Expt possibly include core-excited states [37]. The 8p-2h states with positive parity in addition to the negative-parity states could be at low energy, because the $(fp)^8$ configurations corresponding to ^{48}Cr gain very large binding energy due to α-like four nucleon correlations discussed in the next section. The observed energy levels with $T = 0$ seem to be in a middle situation between the KB3 and FEI results.

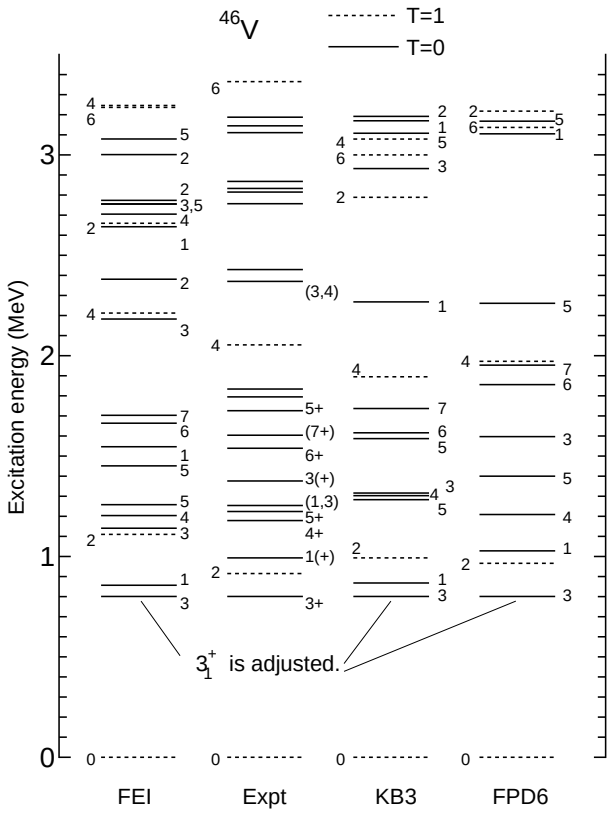

Fig. 3. Energy levels obtained using various effective interactions in ^{46}V, compared with observed ones. Observed levels with unknown spin and parity are also shown.

3.3 ^{48}Cr

The ^{48}Cr nucleus has been attracting notice to the rotational band and backbending. In Fig.4, we illustrate calculated and observed energy levels [33,39–41]. The observed yrast levels, all levels with $J \leq 6$ below 5 MeV and some others above 5 MeV are shown in the column Expt and corresponding levels obtained by the present model are shown in the column Calc. In Table 4, we compare electric quadrupole properties between theory and experiment [39] (the observed value of $B(E2 : 2_1^+ \rightarrow 0_1^+)$ is from Ref. [42]) and also show the full fp shell model result of Caurier *et al.* [16] for comparison.

Our model reproduces satisfactorily well the observed levels of the ground-state band and the backbending at the 12_1^+ level, though there are slight deviations for the 6_1^+, 8_1^+ and 10_1^+ states. The agreement is nearly comparable to that of the full fp shell model calculation with the KB3 interaction [16]. The calculated $E2$ transition probabilities $B(E2 : J \rightarrow J-2)$ in the ground-state band, which are also comparable to those of Caurier *et al.*, correspond well with the observed very large $B(E2)$ values in spite of the lack of the $f_{5/2}$ orbit. This suggests that our interaction including the QQ force is in harmony with the

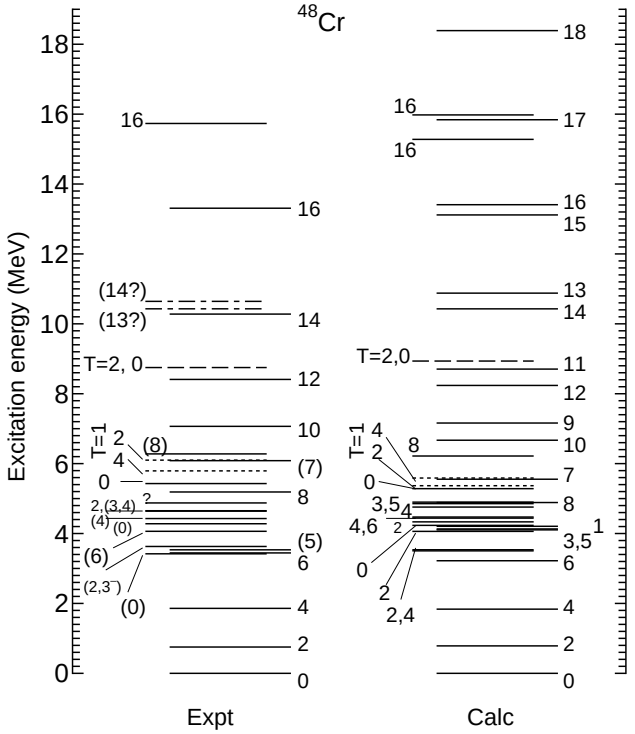

Fig. 4. Calculated and observed energy levels of ^{48}Cr.

collective motion of the ground-state band and yields the large $E2$ transition probabilities. If we add the $f_{5/2}$ orbit to the present model, a smaller effective charge can probably reproduce the observed $B(E2)$ values. The spectroscopic quadrupole moment Q_{spec} indicates the structure change of the ground-state band at 12_1^+, corresponding to the backbending. The relatively large $B(E2)$ values between the states with J=odd and J=even, $B(E2: 11_1 \rightarrow 12_1)$ and $B(E2: 13_1 \rightarrow 12_1)$ at the 12_1^+ state are interesting. Our model predicts that the odd-spin state $(2J-1)_1^+$ lies near above the even-spin state $(2J)_1^+$ when $2J$=10, 12 and 14 but the $(2J-1)_1^+$ state is lower than the $(2J)_1^+$ state when $2J > 14$. The quality of our model will be examined by the experiment on these points.

The present model can give information on high-spin states except the ground-state band. Brandolini *et al.* [39] recently identified an energy level 16^+ at 15.733 MeV. Near there, our model provides two candidates with 16^+. Cameron *et al.* [40] detected two states 13^+ and 14^+ at 10.430 MeV and 10.610 MeV before. One of them possibly corresponds to the 13_1^+ level in the column Calc. The position of the calculated low-lying levels except the yrast states seems to be not so bad. The calculated level density is, however, thicker than that observed until now. The present model has a tendency to give too many non-yrast levels at low energy, as seen in ^{46}V. This could be attributed not only to the insufficiency of the $P_0 + P_2 + QQ + V_{\pi\nu}^{\tau=0}$ interaction but also to the small model space. Since the extension of the model space lowers selectively the

Table 4
Electric quadrupole properties of the yrast states in ^{48}Cr: $B(E2)$ in e^2 fm^4; Q_{spec} and $Q^{(t)}$ in e fm^2.

	Expt.	present work			Caurier *et al.*		
$J \to J'$	$B(E2)$	$B(E2)$	Q_{spec}	$Q_0^{(t)}$	$B(E2)$	Q_{spec}	$Q_0^{(t)}$
$2 \to 0$	321(41)*	217	-29.7	104	228	-29.5	107
$4 \to 2$	329(110)	305	-38.8	104	312	-39.2	105
$6 \to 4$	301(78)	300	-38.9	98	311	-39.7	100
$8 \to 6$	230(69)	285	-40.7	93	285	-38.9	93
$7 \to 5$		92					
$10 \to 8$	195(54)	231	-35.6	83	201	-22.5	77
$9 \to 10$		38					
$\to 7$		124					
$12 \to 10$	167(25)	130	-11.9	62	146	-5.3	
$11 \to 12$		78					
$\to 9$		37					
$\to 10$		9					
$14 \to 12$	105(18)	105	-10.8	55	116		
$13 \to 11$		43					
$\to 12$		43					
$\to 14$		26					
$15 \to 13$		49					
$\to 14$		22					
$16 \to 14$	37(8)	61	-12.6	42	56		
$17 \to 15$		69					
$\to 16$		15					
$18 \to 16$		0.0	-29.2	0.2			
$\to 17$		16					

collective states rather than non-collective states, the full fp shell calculation deserves to be tested.

Figure 4 illustrates the isobaric analogue states, 4^+ and 2^+ with $T = 1$ (dotted lines) and 0^+ with $T = 2$ (dashed line). Our simple interaction including the isoscalar p-n force $V_{\pi\nu}^{\tau=0}$ lays them at roughly good positions, if we neglect the

inverse order of the 4^+ and 2^+ levels in the calculated result.

3.4 ^{48}V

In Fig. 5, we show calculated energy levels of the odd-odd nucleus $^{48}_{23}V_{25}$, compared with observed ones [33,40]. Only the yrast levels and 7 other levels with definitely assigned spin at low energy are shown in the column Expt, and corresponding energy levels obtained by the present model are shown in the column Calc. The present model gives lower energies to the 2_1^+ and 1_1^+ states than the 4_1^+ ground state. The states except the yrast states come to low energy region as compared with the observed ones. We have already stated the overbinding of non-collective states. The $P_0 + P_2 + QQ + V_{\pi\nu}^{\tau=0}$ interaction is still able to describe the yrast band 4_1^+, 5_1^+, 6_1^+ ... 15_1^+ based on the 4_1^+ state as seen in Fig. 5. The correspondence between calculated and observed yrast levels is quite well. The quality is the same as that of the full fp shell model calculation with the KB3 interaction [16]. There is, however, a discrepancy between theory and experiment about the order of the levels 14_1^+ and 15_1^+.

Table 5 shows theoretical and experimental values of $B(E2)$ in ^{48}V. The present results on the $B(E2)$ values agree well with those of the full fp shell model calculation with the KB3 interaction [16], except the 2_1^+ and 4_2^+ states. Although there are little experimental data, our model seems to be able to explain the observed large values of $B(E2)$ between the yrast states 4_1^+, 5_1^+, 6_1^+ etc. to the same extent as the full fp shell model calculation of Caurier *et al.* The calculated results suggest a structure change in the yrast band

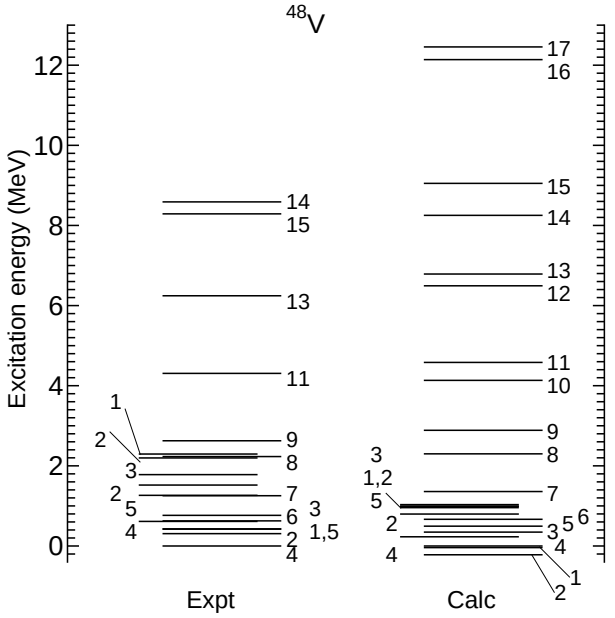

Fig. 5. Calculated and observed energy levels of ^{48}V.

at 8_1^+. The spectroscopic quadrupole moment Q_{spec} changes rapidly from the positive value at the 4_1^+ state to the negative value at the 8_1^+ state. Coincidently, $B(E2: J \to J-1)$ is larger than $B(E2: J \to J-2)$ up to 7_1^+, while $B(E2: J \to J-2)$ is larger than $B(E2: J \to J-1)$ from 8_1^+ till 15_1^+. There seem to be two series of states with even J and odd J connected by the large

Table 5
Quadrupole transition probabilities $B(E2)$ (in e^2 fm^4) and Q_{spec} (in e fm^2) in ^{48}V. The upper part shows calculated $B(E2)$ values of the present work and Caurier *et al.*, compared with observed ones. The lower part shows the results of present work for high-spin yrast states.

	Expt.	present work		Caurier
$J_n \to J'_m$	$B(E2)$	$B(E2)$	Q_{spec}	$B(E2)$
4_1			29.5	
$2_1 \to 4_1$	28.59(17)	105		48.1
$5_1 \to 4_1$	104(42)	183	20.7	209.0
$4_2 \to 4_1$	63(25)	182		28.9
$\to 5_1$	<41	76		32.0
$6_1 \to 5_1$	186(73)	164	-0.3	191.0
$\to 4_1$	46(6)	78		52.0
$5_2 \to 4_2$	<176(124)	34		41.0
$2_2 \to 2_1$	>1.3(19)	4.7		10.7

	present work				
J_1	Q_{spec}	$\to J'_1$	$B(E2)$	$\to J'_1$	$B(E2)$
7_1	-6.5	$\to 5_1$	70	$\to 6_1$	114
8_1	-14.0	$\to 6_1$	138	$\to 7_1$	84
9_1	-15.8	$\to 7_1$	137	$\to 8_1$	66
10_1	-21.3	$\to 8_1$	137	$\to 9_1$	51
11_1	-15.6	$\to 9_1$	128	$\to 10_1$	31
12_1	-23.7	$\to 10_1$	95	$\to 11_1$	22
13_1	-17.7	$\to 11_1$	95	$\to 12_1$	18
14_1	-7.9	$\to 12_1$	24	$\to 13_1$	2.2
15_1	-13.7	$\to 13_1$	48	$\to 14_1$	11
16_1	-18.2	$\to 14_1$	2.3	$\to 15_1$	9.1
17_1	-22.8	$\to 15_1$	1.5	$\to 16_1$	5.7

$B(E2)$ above the 7_1^+ level, which is consistent with the observed strong $E2$ transitions $15_1^+ \rightarrow 13_1^+ \rightarrow 11_1^+ \rightarrow 9_1^+$ (the calculated Q_{spec} values is nearly constant for these states). This is similar to the case of ^{46}V. There is, however, a difference between ^{46}V and ^{48}V in the calculated results. The order of the two levels $(2J)_1^+$ and $(2J+1)_1^+$ is reversed for $2J \geq 8$ in ^{46}V, while it is in order of spin in ^{48}V except 14_1^+ and 15_1^+. Future experiments will judge the quality of our model. The discrepancy between theory and experiment [40] with respect to the order of the two levels 14_1^+ and 15_1^+ should be examined further.

3.5 ^{50}Cr

Let us compare calculated energy levels of ^{50}Cr with observed ones [33,35,39,43] in detail. Figure 6 shows low-lying states below 4 MeV and Fig. 7 illustrates a gross level scheme, mainly the yrast states and high-spin states. In Table 6, we compare electric quadrupole properties between theory and experiment. The observed values of $B(E2)$ are from Refs. [39] (Expt.1) and [35] (Expt.2) and $B(E2: 2_1^+ \rightarrow 0_1^+)$ is from Ref. [44]. The theoretical results of Martínez-Pinedo *et al.* [21] and Zamick *et al.* [19] are listed for comparison.

Figures 6, 7 and Table 6 demonstrate that the present model excellently describes the energies and electric quadrupole properties of the low-spin collective states 0_1^+, 2_1^+, 4_1^+, 6_1^+ and 8_1^+ before the backbending in the ground-state

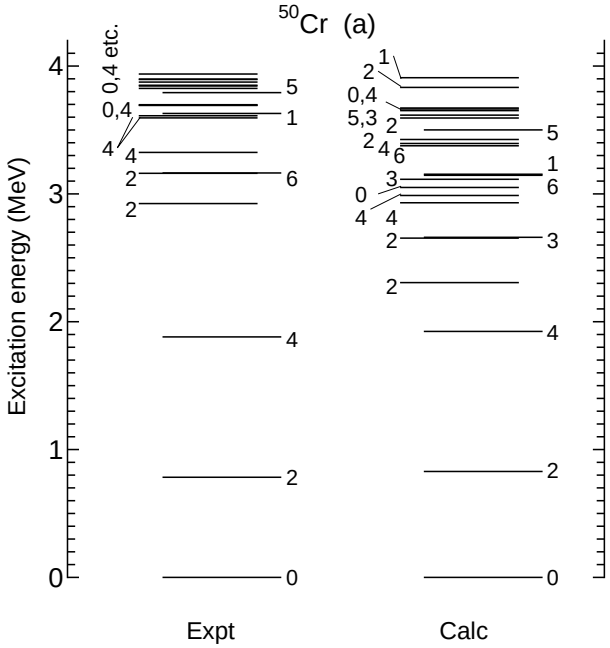

Fig. 6. Calculated and observed energy levels of ^{50}Cr. The states below 4 MeV are shown.

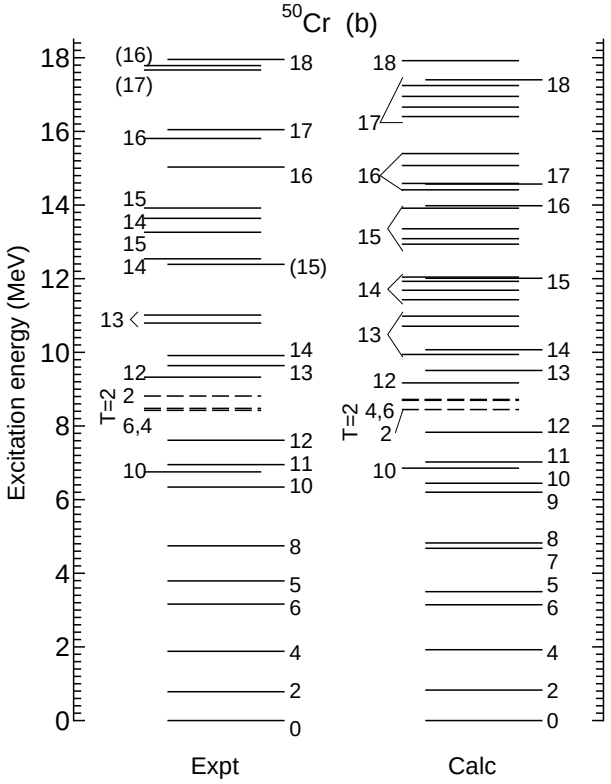

Fig. 7. Calculated and observed yrast levels, high-spin states and $T = 2$ isobaric analogue states of ^{50}Cr.

band. (Remember that the ground-state energy is reproduced very well.) Figure 6, at the same time, reveals the insufficiency of the present model for non-collective states. The calculated low-lying states except the collective states lie lower than the observed levels, though there seems to be a certain correspondence between theory and experiment.

As confirmed in Fig. 7, the correspondence between theory and experiment is very well for the ground-state band, except for the 16^+ level. The calculated $E2$ transition probabilities $B(E2 : J \to J-2)$ in the ground-state band, which are comparable to those of the full fp shell model calculation with the KB3 interaction, well explain the observed $B(E2)$ values except that our model suggests a structure change at 10^+_1 by the small value of $B(E2 : 10^+_1 \to 8^+_1)$. The spectroscopic quadrupole moment Q_{spec}, which is also comparable to that of Martínez-Pinedo *et al.*, abruptly changes to the positive value at 10^+_1 from the negative values up to 8^+_1, indicating the structure change. Our model, on the other hand, reproduces the large value of $B(E2 : 10^+_2 \to 8^+_1)$ as well as the energy of the 10^+_2 state. The nice reproduction of the energy levels 8^+_1, 10^+_1, 10^+_2, 11^+_1, 12^+_1, 12^+_2, 13^+_1 and 14^+_1 manifests that our model describes the backbending phenomenon of the ground-state band well. It is interesting that the $E2$ transition probability $B(E2 : J \to J-1)$ is larger than $B(E2 : J \to J-2)$ for the 11^+_1, 12^+_1 and 13^+_1 states near the backbending.

Table 6
Electric quadrupole properties of the yrast and other states in ^{50}Cr: $B(E2)$ in e^2 fm^4; Q_{spec}, $Q^{(s)}$ and $Q^{(t)}$ in e fm^2.

	$B(E2)$		present work				Martínez *et al.*		Zamic *et al.*	
$J_n \to J'_m$	Expt.1	Expt.2	$B(E2)$	Q_{spec}	$Q_0^{(s)}$	$Q_0^{(t)}$	$B(E2)$	Q_{spec}	$B(E2)$	Q_{spec}
$2_1 \to 0_1$	217±25		215	-29	101	104	193	-27	173	-24.8
$4_1 \to 2_1$	204±57		302	-38	103	103	264	-33	246	-30.0
$6_1 \to 4_1$	235±47		211	-18	44	82	224	-18	215	-15.6
$8_1 \to 6_1$	205±51		200	-25	59	78	200	-17	192	-14.7
$8_2 \to 6_1$			0.3	4.3					0.4	19.5
$10_1 \to 8_1$	72±14	66^{+102}_{-34}	14	47	-108	20	54	30	81	26.5
$\to 8_2$			15						32	
$\to 9_1$			2.7							
$10_2 \to 8_1$	131±26		145	-14					68	12.5
$\to 8_2$			0.7						9.5	
$11_1 \to 9_1$			41	29						
$\to 10_1$			78							
$12_1 \to 10_1$	52±7	0+23	29	17	-37	29	30	13	69	13.0
$\to 10_2$			9						12	
$\to 11_1$			51							
$12_2 \to 10_1$			1.0	-17					0.0	-6.6
$\to 10_2$			20						51	
$13_1 \to 11_1$	>5	>30	42	8.6						
$\to 12_1$			49							
$14_1 \to 12_1$	43±7	31±7	52	10	-22	39	60	8	67	8.2
$\to 13_1$			13							
$15_1 \to 13_1$	>10	>21	11	-6.4						
$\to 14_1$			0.8							
$16_1 \to 14_1$	>10		7.8	7.6	-17	15	3	10	.8	-8.7
$\to 15_1$			3.3							
$17_1 \to 15_1$		>66	67	-6.2						
$\to 16_1$			14							
$18_1 \to 16_1$	50±20		0.5	-25	53	3.9	76	9	83	-8.0
$\to 17_1$			17							

There is a disagreement between theory and experiment on the energies of the 16_1^+ and 17_1^+ states and $B(E2: 18_1^+ \rightarrow 16_1^+)$. A little possibility that the two levels 16^+ and 17^+ observed at 15.032 MeV and 16.048 MeV are not the yrast states remains. Our model predicts a bundle of levels with the same J near each high-spin yrast level. Actually, there are calculated energy levels corresponding well to the observed levels with 10^+, 12^+, 13^+, 14^+ and 15^+ in addition to the yrast levels. The observed 16^+ and 17^+ states at 15.032 MeV and 16.048 MeV have such candidates at the same energy region in the calculated energy spectra. The calculated values $B(E2: 18_1^+ \rightarrow 16_1^+) = 0.5$ and $B(E2: 18_2^+ \rightarrow 16_1^+) = 1.7$ in e^2 fm^4 are much smaller than the observed one. The absence of the $f_{5/2}$ orbit may have the influence on the energies and $B(E2)$ of the high-spin states 16^+, 17^+ and 18^+, in the present model.

Our model reproduces the isobaric analogue states 6^+, 4^+ and 2^+ with T=2 (broken lines) at good energy, though the order of the calculated levels $(6^+, 4^+)$ and 2^+ is reverse to that of the observed ones. This is a nice work of the isoscalar p-n force $V_{\pi\nu}^{\tau=0}$.

3.6 ^{50}Mn

A recent experiment by Svensson *et al.* [45] identified high-spin states in the $N = Z$ odd-odd nucleus $^{50}_{25}\mathrm{Mn}_{25}$. We compare the energy scheme obtained by the present model with the observed one in Fig. 8. Like ^{48}V, our model lays another T=0 state (1_1^+) at lower energy than the 5_1^+ state which is the lowest T=0 state in experiment. Moreover, these two calculated states 1_1^+ and 5_1^+ lie

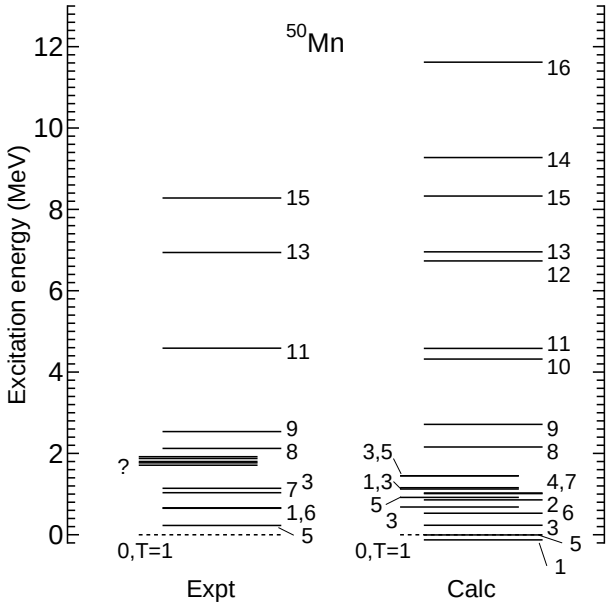

Fig. 8. Calculated and observed energy levels of ^{50}Mn.

lower than the ground state 0_1^+ with T=1. The discrepancy between theory and experiment for the T=0, 5_1^+ level, however, is only 0.23 MeV. For such a simple model, the obtained energies of the T=1, 0^+ and T=0, 5_1^+ states are rather satisfactory. We see again that the calculated non-collective states except the yrast states lie lower than the observed ones.

Table 7
Electric quadrupole properties of the yrast states in ^{50}Mn: $B(E2)$ in e^2 fm^4 and various Q values in e^2 fm^2.

	present work				Svenssen *et al.*			
$J \to J'$	$B(E2)$	Q_{spec}	$Q_0^{(s)}$	$Q_0^{(t)}$	$B(E2)$	Q_{spec}	$Q_0^{(s)}$	$Q_0^{(t)}$
$3 \to 1$	259	-33	-19		240			
5		59	102			57	98	
$6 \to 5$	294	32	103	99	258	32	102	93
$7 \to 6$	301	13	94	92	251	14	100	84
$\to 5$	39			90	42			92
$8 \to 7$	276	3.4	191	90	140	5	285	64
$\to 6$	89			95	74			87
$9 \to 8$	217	-5.6	78	84	142	-0.6	9	68
$\to 7$	127			95	133			97
$10 \to 9$	177	-8.1	59	81				
$\to 8$	128			85				
$11 \to 9$	97	5.4	-28	69	130	0.5	-2.6	80
$\to 10$	62			51				
$12 \to 11$	119	-0.4	1.5	76				
$\to 10$	73			57				
$13 \to 11$	83	-1.5	5.6	58	99	6	-23	64
$\to 12$	61			59				
$14 \to 13$	69	-1.8	6.2	65				
$\to 12$	43			41				
$\to 15$	0.0							
$15 \to 13$	27	33	-105	32	47	25	-80	41
$16 \to 15$	43	14	-42	58				
$\to 14$	47			41				

It is impressive that the observed T=0 yrast band on the 5_1^+ state is reproduced so well by our simple model. The correspondence between theory and experiment is better than that of the full fp shell model calculation using the KB3 interaction and single-particle energies taken from ^{41}Ca [45]. Calculated $E2$ transition probabilities between the yrast states are compared with those of Ref.[45] in Table 7. The $B(E2)$ values in the present work are larger up to 9_1^+ and smaller above 10_1^+ than those of Ref. [45].

The theoretical $B(E2)$ values between the yrast states in ^{50}Mn show a different feature from those in ^{46}V and ^{48}V. Namely, every $B(E2 : J \to J-1)$ is larger than $B(E2 : J \to J-2)$ except the 15_1^+ state in ^{50}Mn, while the relative magnitudes of $B(E2 : J \to J-1)$ and $B(E2 : J \to J-2)$ are reversed above 7_1^+ corresponding to the structure change in ^{46}V and ^{48}V. In ^{50}Mn, the spectroscopic quadrupole moment Q_{spec} changes one after another but the intrinsic quadrupole moment $Q_0^{(t)}$ keeps relatively large values up to high spin. There is probably a delicate difference between ^{46}V and ^{50}Mn which are cross-conjugate systems $(f_{7/2})^{6p}$ and $(f_{7/2})^{6h}$ within the single j model space. The present result suggests a considerably large contribution of the upper orbits $p_{3/2}$ and $p_{1/2}$ in ^{50}Mn. Our model yields different level schemes in ^{46}V and ^{50}Mn. The inverse order of the levels $(2J)_1^+$ and $(2J+1)_1^+$ happens above $2J = 8$ in ^{46}V but happens only at $2J = 14$ in ^{50}Mn. This interesting difference will be examined by detecting the even-J high-spin states.

4 Discussions

4.1 Dependence of the calculated results on the model

@We have seen the success of the present model in the small model space $(f_{7/2}, p_{3/2}, p_{1/2})$. To see the dependence on the model space, we made calculations with our interaction in the full fp shell for ^{44}Ti where the calculations are easy. We took $\epsilon(f_{5/2})$=4.88 MeV from ^{41}Ca and changed the force strengths as little as possible so as to reproduce the observed energy levels of ^{44}Ti, i.e., $g_0 = 0.42(42/A)$, $\chi' = 0.29(42/A)^{5/3}$, and g_2 and k^0 being unchanged. Obtained energy levels (column B) are compared with those in the $(f_{7/2}, p_{3/2}, p_{1/2})$ space (column A) and also with the results obtained using the FPD6 [14] and KB3 interactions in the full fp space, in Fig. 9. This figure teaches that the extension of the model space to the full fp space modifies little the energy levels of the collective states in our model. This is probably true for the collective states of A=46, 48 and 50 nuclei, as guessed from the successful results in Sec. III. We shall see the reason in the next subsection.

According to Fig. 9, our interaction FEI is roughly comparable to the FPD6

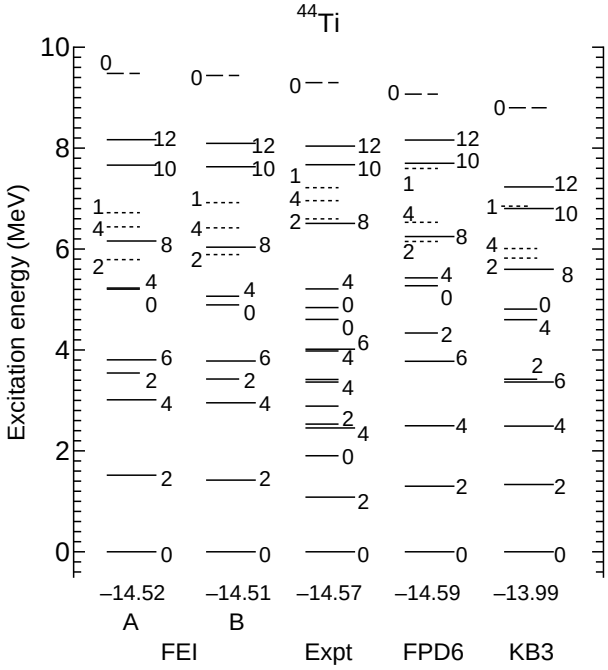

Fig. 9. Energy levels obtained using various effective interactions in ^{44}Ti, compared with observed levels. The ground-state energy is written below every 0^+_1 level in MeV. The dotted lines denote the $T = 1$ states and dashed lines denote the $T = 2$, 0^+ state. The space A is $(f_{7/2}, p_{3/2}, p_{1/2})$ and B is the full fp space.

and KB3 interactions also in ^{44}Ti. The KB3 interaction yields rather compressed energy levels for the ground-state band and a shallow binding energy. This could be attributed to the lack of the $g_{9/2}$ orbit which is included in the model space of the original Kuo-Brown (KB) interaction [7]. If the $g_{9/2}$ orbit is added, the additional interactions such as the pairing force will lower the low-lying collective states 0^+_1, 2^+_1 ... and recover the binding energy. This situation presents a contrast to the success of the KB3 interaction in the A=46, 48 and 50 nuclei.

The extension of the model space, of course, changes the wave functions. Table 8 lists the $B(E2 : J^+_1 \rightarrow (J-2)^+_1)$ values calculated in the $(f_{7/2}, p_{3/2}, p_{1/2})$ space and full fp space, which are compared with the observed $B(E2)$ values and those obtained by the α-cluster model [48]. The extension of the model space enlarges the $B(E2)$ values between the most collective states 2^+_1 and 4^+_1, when our interaction is used. The same does not happen for the realistic effective interactions FPD6 and KB3. The two interactions rather reduce the $B(E2)$ values between the 2^+_1, 4^+_1, 6^+_1 and 8^+_1 states. An advantage of the α-cluster model [48] was the reproduction of the large $B(E2)$ values without the effective charge as compared with the reduced $B(E2)$ values of the shell models using the realistic effective interactions. The shell model using the FEI yields the $B(E2)$ values comparable with the α-cluster model, though the former employs the effective charge $e_{eff} = 0.5e$. The ^{44}Ti nucleus is more

Table 8
Dependence of $B(E2: J_1^+ \to (J-2)_1^+)$ on model spaces and effective interactions in ^{44}Ti. The space A is $(f_{7/2}, p_{3/2}, p_{1/2})$ and B is the full fp space. The $B(E2)$ values obtained by the α-cluster model is also shown.

	FEI		Expt.	FPD6		KB3		α-
J	A	B		A	B	A	B	cluster
2	102	103	120±37	80	60	73	64	107
4	125	134	277±55	101	72	94	75	146
6	82	74	157±28	99	63	91	57	140
8	77	73	>18	91	58	84	50	118
10	76	67	138±28	79	67	70	62	75
12	52	52	40±8	50	52	44	47	34

or less in an α-like four-nucleon correlated state outside the doubly-closed-shell ^{40}Ca core [49]. The large $B(E2)$ values are related to the α-like four-nucleon correlations. The $P_0 + P_2 + QQ + V_{\pi\nu}^{\tau=0}$ interaction, which is suitable for the description of the nuclear collective motions (the quadrupole vibration and deformation), is considered to have an affinity also for the α-like four-nucleon correlations [50] as compared with the FPD6 and KB3 interactions as seen in Table 8. Anyhow, our interaction including the QQ force can give larger $B(E2)$ values than the FPD6 and KB3 interactions, when the same model space is used. In the configuration $(f_{7/2}, p_{3/2}, p_{1/2})^8$ for ^{48}Cr, for instance, the KB3 interaction gives $B(E2: 4_1^+ \to 2_1^+) = 196\ e^2\ \mathrm{fm}^4$, while the FEI gives $B(E2: 4_1^+ \to 2_1^+) = 305\ e^2\ \mathrm{fm}^4$. Thus our interaction in the smaller model space $(f_{7/2}, p_{3/2}, p_{1/2})$ reproduces large $B(E2)$ values comparable to the FPD6 and KB3 interactions in the full fp space, in the A=46, 48 and 50 nuclei. If we extend the model space using our interaction, a smaller effective charge will serve in the A=46-50 nuclei.

There is another sign that the three interactions FEI, FPD6 and KB3 give different wave functions. For ^{44}Ti, the expectation values of nucleon number in respective orbits of the fp space are as follows: $n_{7/2}$=3.082, $n_{3/2}$=0.701, $n_{1/2}$=0.103, $n_{5/2}$=0.114 for FEI; $n_{7/2}$=3.061, $n_{3/2}$=0.464, $n_{1/2}$=0.124, $n_{5/2}$=0.351 for FPD6; $n_{7/2}$=3.367, $n_{3/2}$=0.262, $n_{1/2}$=0.085, $n_{5/2}$=0.286 for KB3. The contribution of the $p_{3/2}$ orbit is large in FEI. Nucleons are distributed over all the orbits most in FPD6. It should be noticed that interactions related to the $f_{7/2}$ orbit are strengthened in KB3 by the modification from the KB interaction [16], resulting in the large value of $n_{7/2}$.

The results of calculations depend also on the single-particle energies. We examined the dependence by shell model calculations using Kuo-Brown's single-particle energies, $\epsilon_{7/2}$=0.0, $\epsilon_{3/2}$=2.1 and $\epsilon_{1/2}$=3.9 in MeV. In Table 9, calcu-

lated energies and $B(E2)$ for the ground-state bands of ^{46}Ti and ^{48}Cr are compared with those of Sec. III (where $\epsilon_{7/2}$=0.0, $\epsilon_{3/2}$=1.94 and $\epsilon_{1/2}$=3.61 in MeV). Table 9 says that the change of the single-particle energies tried here does not significantly affect the energies and $B(E2)$. We, therefore, need not change the basic understanding in Sec. III, as long as we use ordinary single-particle energies.

Table 9
Effects of varying the single-particle energies on the excitation energies E_x (or ground-state energies E_{gs}) and $B(E2)$ values. The single-particle energies $(\epsilon_{7/2}, \epsilon_{3/2}, \epsilon_{1/2})$ are taken from ^{41}Ca in I and are Kuo-Brown's in II, respectively.

	E_x or (E_{gs})		$B(E2: J \to J-2)$	
$A\ J_1^\pi$	I	II	I	II
^{46}Ti 0_1^+	(-20.169)	(-19.987)		
2_1^+	1.110	1.133	119	116
4_1^+	2.212	2.220	159	152
6_1^+	3.237	3.198	141	133
8_1^+	4.984	4.934	126	119
10_1^+	6.570	6.479	104	100
11_1^+	7.548	7.420	51	48
12_1^+	8.177	8.049	53	51
14_1^+	10.491	10.330	26	25
^{48}Cr 0_1^+	(-32.380)	(-32.131)		
2_1^+	0.785	0.802	217	211
4_1^+	1.837	1.847	306	297
6_1^+	3.222	3.217	301	287
7_1^+	5.554	5.524	92	89
8_1^+	4.887	4.866	285	274
10_1^+	6.670	6.606	232	219
12_1^+	8.238	8.095	130	127
13_1^+	10.878	10.770	43	32
14_1^+	10.429	10.248	105	103

4.2 Characteristics of the interaction matrix elements

The effective interactions can be directly checked in ^{42}Sc. In Fig. 10, we compare energy levels obtained using the three interactions (FEI, FPD6 and KB3) in ^{42}Sc with observed energy levels, where the model space $(f_{7/2}, p_{3/2}, p_{1/2})$ is employed for FEI. This figure shows that the isoscalar ($T = 0$) p-n interactions of FEI are best but the isovector ($T = 1$) interactions of FEI are worst among the three interactions. We now understand the reason why our interaction is not good for the Ca isotopes where only the isovector interactions take action. Probably, the isovector interactions play dominant roles in low-lying states of nuclei with n_p=1 or n_n=1. The success of our interaction FEI for the collective states in the A=46, 48 and 50 nuclei with $n_p \geq 2$ and $n_n \geq 2$ suggests leading roles of the isoscalar p-n interactions there.

The compression of the $T = 1$ energy levels $(0^+, 2^+, 4^+, 6^+)$ in the KB3 result of Fig. 10 is due to the lack of the $g_{9/2}$ orbit (compare with the figure of Ref. [7]), as mentioned in the previous subsection. The KB3 interaction lays the $T = 0$ states $(7^+, 1^+, 5^+, 3^+)$ lower than the FPD6. This is caused by the modification of interaction matrix elements from the original KB interaction [7] to the KB3 [16], where the most important modification is to strengthen the isoscalar p-n interactions.

In Table 10, we list typical interaction matrix elements of the four interactions FPD6, KB, KB3 and FEI. For FEI, the force parameters fixed in ^{44}Ti

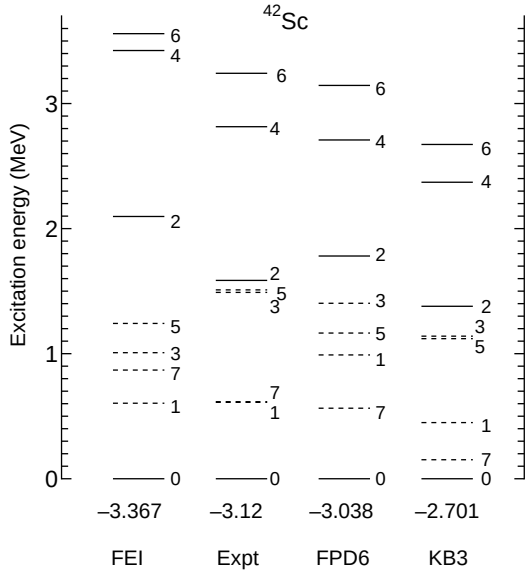

Fig. 10. Energy levels obtained using various effective interactions in ^{42}Sc, compared with observed levels. The ground-state energy is written below every 0_1^+ level in MeV. The solid lines denote the $T = 1$ states and dotted lines denote the $T = 0$ states.

are applied to the $A = 42$ system, i.e., $g_0 = 0.42$, $g_2 = 0.36$, $\chi' = 0.30$ and $k^0 = 2.23$ in MeV. Let us denote diagonal matrix elements as $V(abJT) = \langle abJT|V|abJT\rangle$. The KB3 interaction enlarges $V(f_{7/2}f_{7/2}J = odd, T = 0)$ more than $V(f_{7/2}f_{7/2}J = even, T = 1)$, especially $V(f_{7/2}f_{7/2}J = 1, T = 0)$ and $V(f_{7/2}f_{7/2}J = 3, T = 0)$ as well as $V(f_{7/2}rJ, T = 0)$ with $r = (p_{3/2}, p_{1/2}, f_{5/2})$. These modifications bring the KB3 interaction a little near to the FEI. In our interaction FEI, the $V_{\pi\nu}^{\tau=0}$ force strengthens just the isoscalar ($T = 0$) p-n interactions, and the matrix elements $V(f_{7/2}f_{7/2}J = 1, T = 0)$ and $V(f_{7/2}f_{7/2}J = 3, T = 0)$ are comparable with $V(f_{7/2}f_{7/2}J = 7, T = 0)$, which makes the 1^+ state lowest among the $T = 0$ states of ^{42}Sc.

The modification of the centroids of interaction matrix elements in the KB3 interaction is discussed in terms of the monopole Hamiltonian in Refs. [16,51]. That discussion is intimately related to the roles of the $V_{\pi\nu}^{\tau=0}$ force. We have shown in the previous papers [30,31] that the $V_{\pi\nu}^{\tau=0}$ force plays an essential role for reproducing the binding energy and symmetry energy in a very wide range of nuclei. The $V_{\pi\nu}^{\tau=0}$ force which has a simple and definite form (see Eq. (8) or (9)) can play the part for Zuker's monopole Hamiltonian. According to Dufour and Zuker [27], the residual interactions after extracting the monopole Hamiltonian or the $V_{\pi\nu}^{\tau=0}$ force must resemble the $P_0 + P_2 + QQ$ force.

The J-independent isoscalar p-n force $V_{\pi\nu}^{\tau=0}$ gives the average value -2.23 MeV to the diagonal matrix elements $V(abJ, T = 0)$ (see Table 10). The absolute values of $V(f_{7/2}p_{3/2}J, T = 0)$ of our interaction FEI are larger than those of the realistic effective interactions. The FPD6 and KB3 interactions have very large matrix elements $V(f_{7/2}f_{5/2}J, T = 0)$, to which the matrix elements of FEI are comparable. The centroid of $V(f_{7/2}f_{5/2}J, T = 0)$ is -1.846 for FPD6, -1.934 for KB3 and -2.241 for FEI. Seeing the large diagonal matrix elements, one naturally hesitates to omit the $f_{5/2}$ orbit from the model space and hence deals with the full fp shell space. Why the truncated space $(f_{7/2}, p_{3/2}, p_{1/2})$ works well for the $P_0 + P_2 + QQ + V_{\pi\nu}^{\tau=0}$ interaction? The secret is in a special work of $V_{\pi\nu}^{\tau=0}$. The J-independent p-n force $V_{\pi\nu}^{\tau=0}$, which is a function of only the number and isospin of valence nucleons in Eq. (8), is independent of the model space in fact. The average contribution of $V(f_{7/2}f_{5/2}J, T = 0)$ is equivalently taken into account in our model. The residual interactions excluding $V_{\pi\nu}^{\tau=0}$ are, of course, desired to be taken up. The inclusion of the $f_{5/2}$ orbit will improve wave functions and $B(E2)$ as seen in the previous subsection. There are large off-diagonal matrix elements $\langle f_{7/2}f_{7/2}J, T = 0|V|f_{7/2}f_{5/2}J, T = 0\rangle$ and $\langle f_{7/2}f_{7/2}J, T = 0|V|f_{5/2}f_{5/2}J, T = 0\rangle$ in the realistic effective interactions. Their effects on the energies of low-lying states, however, may be secondary as guessed from our results.

We have seen the defects of the present model on non-collective states and also the insufficiency of the isovector interactions. The present interaction remains room for improvement, which could be made by comparing with the

Table 10
Comparison of interaction matrix elements $\langle abJT|V|cdJT\rangle$ between various effective interactions. The orbits are labeled by numbers, 1: $f_{7/2}$, 2: $p_{3/2}$, 3: $p_{1/2}$, 4: $f_{5/2}$.

a b c d	J, T	FPD6	KB	KB3	FEI
1 1 1 1	1, 0	-0.177	-0.525	-1.175	-2.680
	3, 0	-0.499	-0.208	-0.858	-2.257
	5, 0	-1.046	-0.502	-0.852	-1.939
	7, 0	-2.474	-2.199	-2.549	-2.490
1 1 1 1	0, 1	-2.268	-1.807	-1.917	-2.236
	2, 1	-0.888	-0.785	-1.095	-0.812
	4, 1	-0.144	-0.087	-0.197	0.185
	6, 1	0.168	0.226	0.116	0.185
1 2 1 2	2, 0	0.003	-0.298	-0.593	-2.552
	3, 0	-0.823	-0.604	-0.904	-2.178
	4, 0	-0.547	-0.164	-0.464	-1.763
	5, 0	-2.522	-2.165	-2.465	-2.801
1 3 1 3	3, 0	-1.824	-1.484	-1.784	-2.230
	4, 0	-0.787	-0.746	-1.046	-2.230
1 4 1 4	1, 0	-4.665	-3.621	-3.921	-2.716
	2, 0	-2.950	-2.731	-3.031	-2.427
	3, 0	-1.263	-0.985	-1.285	-2.207
	4, 0	-2.188	-1.886	-2.186	-1.919
	5, 0	-0.008	-0.112	-0.412	-2.019
	6, 0	-2.402	-2.217	-2.517	-2.490
1 1 1 4	1, 0	1.977	1.894	1.894	-0.130
	3, 0	1.322	1.005	1.005	-0.172
	5, 0	1.307	0.901	0.901	0.042
1 1 4 4	1, 0	2.080	1.071	1.071	-0.061
	3, 0	1.260	0.517	0.517	0.004
	5, 0	0.596	0.170	0.170	0.047

realistic effective interactions. Another way may be to add hexadecapole and hexadecapole-hexadecapole forces (octupole and octupole-octupole forces for negative-parity states) as an extension of the $P_0 + P_2 + QQ$ force.

4.3 Properties of the yrast bands in A=46, 48 and 50 nuclei

In order to look at the structure of the yrast bands in A=46, 48 and 50 nuclei from a different angle, we illustrate the spin-energy relation in Figs. 11, 12 and 13. We clearly see the good applicability of the $P_0 + P_2 + QQ + V_{\pi\nu}^{\tau=0}$ interaction to the collective yrast states in these nuclei. The rotational behavior and backbending in the ground-state bands in even-even nuclei are well reproduced. It is interesting that in ^{50}Cr (Fig. 13) the J=odd line touches the ground-state band with J=even near 11_1^+ where the backbending occurs and the values of $B(E2 : J \rightarrow 11_1^+)$ become large (Table 6). The staggering gait depending on odd spin and even spin observed in the $T = 0$ yrast bands of the odd-odd nuclei is almost traced by our model. We have already indicated that the magnitudes of staggering are not the same in the cross-conjugate nuclei (within the $f_{7/2}$ space) ^{46}V and ^{50}Mn. Figure 14 shows that the $T = 0$ yrast bands of ^{46}V and ^{50}Mn do not resemble at low spin but resemble at J=odd high spin. This suggests the dominant contribution of the $f_{7/2}$ orbit in the high-spin states of ^{46}V and ^{50}Mn.

Figures 11, 12 and 13 suggest that there are similarities between the ground-states bands of the even-even nuclei ^{46}Ti, ^{48}Cr and ^{50}Cr, and between the yrast bands of the odd-odd nuclei ^{46}V, ^{48}V and ^{50}Mn. In Fig. 14, the observed yrast bands in these nuclei are compared in a sheet of drawing. The slopes at the beginning of the bands resemble in the even-even nuclei and also in the

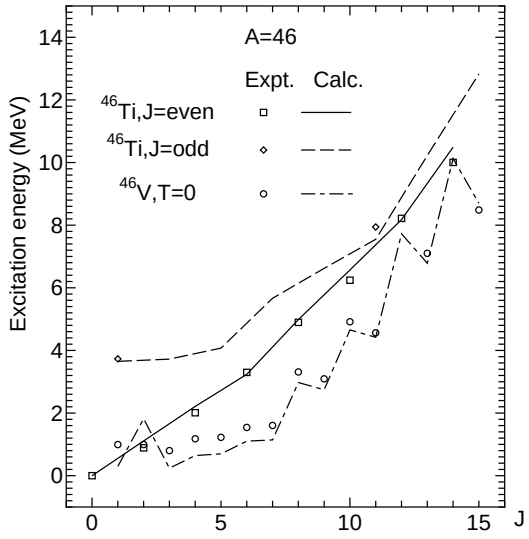

Fig. 11. Spin-energy relation in the yrast bands of ^{46}Ti and ^{46}V.

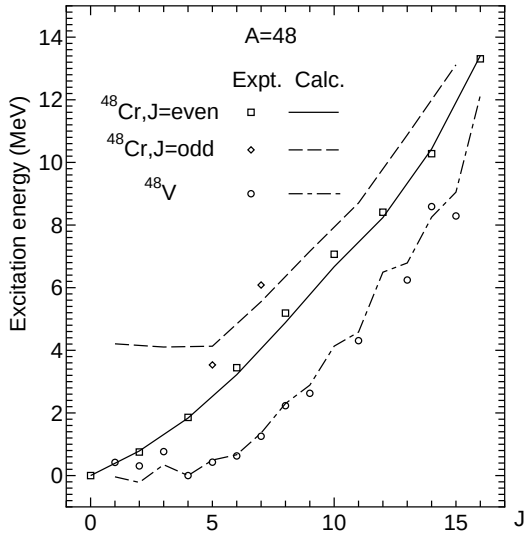

Fig. 12. Spin-energy relation in the yrast bands of ^{48}Cr and ^{48}V.

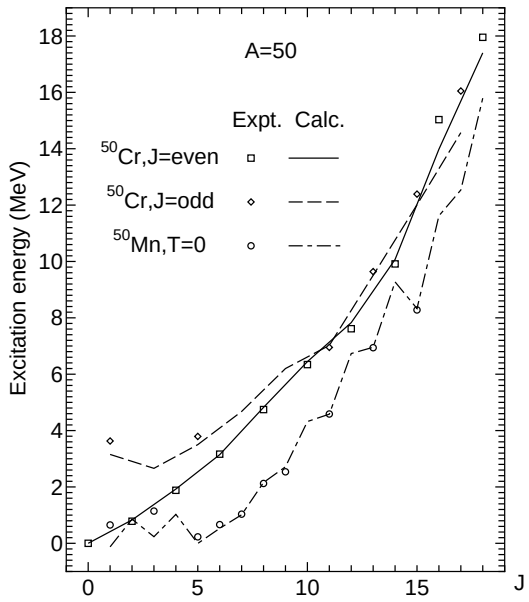

Fig. 13. Spin-energy relation in the yrast bands of ^{50}Cr and ^{50}Mn.

odd-odd nuclei ^{48}V and ^{50}Mn. This implies a similar mechanism of excitation in low-lying collective states of the even-even or odd-odd systems, which is considered to be the nuclear rotation [54–57,28].

The $N = Z$ odd-odd nuclei ^{46}V and ^{50}Mn have $T = 1$ and $T = 0$ bands as the lowest and second lowest bands. (Our Hamiltonian gives the same energies to the $T = 1$ states of ^{46}Ti and ^{46}V (^{50}Cr and ^{50}Mn). The $T = 1$ band observed in ^{46}V or ^{50}Mn, actually, corresponds well to that observed in ^{46}Ti or ^{50}Cr.) Recently, a band crossing which is different from the ordinary one caused by the spin alignment of a high j neutron or proton pair was observed in a heavy $N = Z$ nucleus ^{74}Rb [46]. The crossing frequency which corresponds to $J = 5$

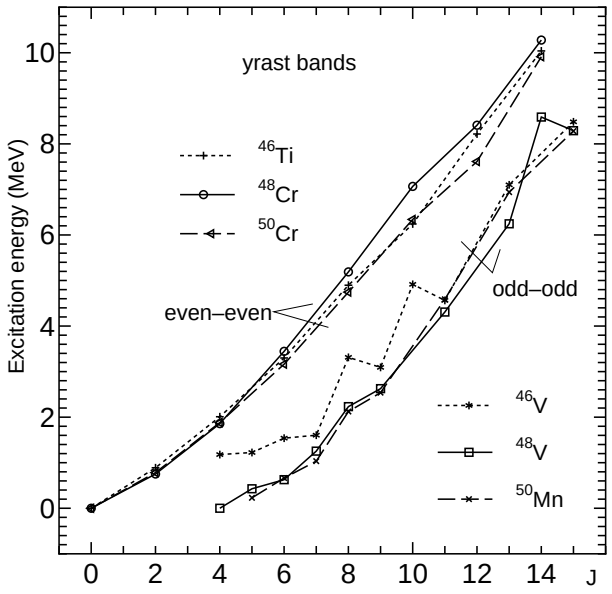

Fig. 14. Similarity between the observed yrast bands in A=46, 48 and 50 nuclei.

or $J = 7$ is smaller than that in the ordinary band crossing. This phenomenon can be interpreted to be the crossing of the $T = 1$ and $T = 0$ bands [46,47,25]. Figures 11 and 13 show a similar behavior in ^{46}V and ^{50}Mn, where the $T = 0$ band appears to cross the $T = 1$ band near $J = 2$. We can suppose a similar situation for the $N = Z$ odd-odd nuclei both in the beginning and middle regions of fpg shell. It is interesting that the crossing frequency in the former region is smaller than that in the latter where nuclei are considered to be certainly deformed.

The backbending phenomena in ^{48}Cr and ^{50}Cr have been studied by the cranked Hartree-Fock-Bogoliubov method [54–57]. A typical interaction for studying the rotation of deformed nucleus by the cranking approach is just the P_0+QQ force which is the main part of our residual interactions excluding the $V_{\pi\nu}^{\tau=0}$ force. It was shown by the projected quasi-particle shell model in the Nilsson base [6] that the P_0+P_2+QQ force successfully describes not only the rotational band in medium-heavy nuclei [5] but also the backbending in ^{48}Cr [28]. The study of Ref. [28] indicates that the P_0+P_2+QQ force is comparable to the realistic effective interaction KB3 in reproducing the rotational band of ^{48}Cr. It should be noticed here that the $P_0 + P_2 + QQ$ force without the p-n force $V_{\pi\nu}^{\tau=0}$ cannot well reproduce the binding energy, and the p-n interactions as well as like-nucleon interactions are taken into account in our P_0+P_2 force. The $P_0 + P_2 + QQ + V_{\pi\nu}^{\tau=0}$ interaction is, therefore, a very suitable interaction to investigate the rotational band and its backbending in the $N \approx Z$ fp shell region, in parallel with the shell model approach.

One of the key words to understand the excitation mechanism at the beginning of the fp shell nuclei seems to be α-like four-nucleon correlations [49]. The

^{44}Ti nucleus is an α-like correlated state outside the ^{40}Ca core. The ^{48}Cr nucleus, in zero order approximation, is described as a correlated state of two α-like clusters (quartets) $\sum_I \psi_I (\alpha^\dagger_{I,T=0})^2 |^{40}\mathrm{Ca}\rangle$ where $\alpha^\dagger_{IM,T=0}$ being the lowest-energy Tamm-Dancoff modes of four nucleons with spin IM and $T = 0$ [52]. The approximate description gives the ground-state energy -32.05 MeV against the exact energy -32.38 MeV in the present model. Within the single $j = f_{7/2}$ shell model, the states of $A = 4n+2$ nuclei are roughly approximated as follows [50,53]:

$$
\begin{aligned}
|^{46}\mathrm{Ti} : J^+_1\rangle &\approx \frac{1}{\sqrt{C_1}} A^\dagger_{0011}(f_{7/2}f_{7/2})|^{44}\mathrm{Ti} : J^+_1\rangle \quad (J = 0, 2), \\
|^{50}\mathrm{Cr} : J^+_1\rangle &\approx \frac{1}{\sqrt{C_2}} A^\dagger_{0011}(f_{7/2}f_{7/2})|^{48}\mathrm{Cr} : J^+_1\rangle \quad (J = 0, 2),
\end{aligned} \tag{16}
$$

where C_1 and C_2 are normalization constants. The overlaps of the approximate states (16) with the exact states are more than 0.98 for $J = 0$ and are more than 0.90 for $J = 2$. In other words, the excitation $0^+_1 \to 2^+_1$ in ^{46}Ti and ^{50}Cr resembles the excitation $0^+_1 \to 2^+_1$ in ^{44}Ti and ^{48}Cr, respectively. The excitation $0^+_1 \to 2^+_1$ in ^{44}Ti is the change of four nucleon structure $\alpha^\dagger_{I=0,T=0} \to \alpha^\dagger_{I=2,T=0}$. A similar change of structure is possibly dominant in the excitation $0^+_1 \to 2^+_1$ in ^{48}Cr. We can suppose a common excitation mechanism induced by the α-like four-nucleon correlations in ^{46}Ti, ^{48}Cr and ^{50}Cr. We have already discussed the intimate relation of our interaction $P_0 + P_2 + QQ + V^{\tau=0}_{\pi\nu}$ to the α-like four-nucleon correlations in Ref. [50]. The $P_0 + P_2 + QQ + V^{\tau=0}_{\pi\nu}$ interaction having strong p-n interactions may underlie commonly in the nuclear rotation and α-like four-nucleon correlations in the fp shell nuclei.

5 Concluding remarks

We have applied a functional effective interaction extended from the pairing plus QQ force by adding the J-independent isoscalar p-n force $V^{\tau=0}_{\pi\nu}$ and quadrupole pairing force to ^{46}Ti, ^{46}V, ^{48}V, ^{48}Cr, ^{50}Cr and ^{50}Mn. The exact shell model calculations in the truncated model space $(f_{7/2}, p_{3/2}, p_{1/2})$ demonstrate the usefulness of the interaction for the yrast states in these nuclei with $n_p \geq 2$ and $n_n \geq 2$. The model reproduces well the experimental binding energies, energy levels of the yrast states and $B(E2)$ between them. We have also analyzed the relationship between our interaction and the realistic effective interactions KB3 and FPD6. The analysis clarified the reason why the truncated model space works well especially for our interaction. This work as well as the previous ones [29–31] supports that an important part of nucleon-nucleon interactions can be written as $V^{\tau=0}_{\pi\nu}$. The foundation of the p-n force $V^{\tau=0}_{\pi\nu}$ could be discussed in the framework of the HF theory.

The good reproduction of the yrast states made it possible to discuss their structure in the A =46, 48 and 50 nuclei. We have given some predictions about the energy levels and characteristic variations of $B(E2)$ in the yrast bands, in these nuclei. The extended $P_0 + QQ$ interaction is excel in describing the collective nature of nuclei, and is expected to be most suitable for studying the rotational properties of the yrast bands. The backbending phenomena in ^{48}Cr and ^{50}Cr, which are well described in terms of the shell model with our interaction, can be investigated by a cranking model with the same interaction. The $P_0+P_2+QQ+V_{\pi\nu}^{\tau=0}$ interaction composed of typical forms of forces is also useful for the study of competition between the $T = 0$ and $T = 1$ p-n pairing and like-nucleon pairing which is one of current topics. There is a sign that the $P_0+P_2+QQ+V_{\pi\nu}^{\tau=0}$ interaction has an affinity for the α-like four-nucleon correlations important in $N \approx Z$ nuclei.

The success of the extended $P_0 + QQ$ interaction by means of the exact shell model gives strong evidence that the extended picture of the pairing plus QQ force model holds in lighter nuclei. This supports the discussion by the projected quasi-particle shell model [5,6,28] that the P_0+P_2+QQ interaction describes well the rotational states not only in medium-heavy nuclei but also in the fp shell nucleus ^{48}Ca. We can probably say that the success of the pairing plus QQ force model in heavier nuclei with $N > Z$ did not depend on approximate treatments made there. Our calculations in this paper and others [29–31] clarified the essential role of the p-n force $V_{\pi\nu}^{\tau=0}$ in the binding energy. If $V_{\pi\nu}^{\tau=0}$ is added to the treatment of the pairing plus QQ plus quadrupole force model in $N > Z$ nuclei, binding energies will be well reproduced too.

The present model, however, is not sufficiently good for non-collective states except the yrast states and for nuclei with $n_p \leq 1$ or $n_n \leq 1$. One cause may be attributed to the absence of the $f_{5/2}$ orbit in the present calculations and another to the insufficiency of the isovector interactions which take action in like-nucleon systems. The present interaction remains room for improvement. One way to improve it is to add hexadecapole and hexadecapole-hexadecapole forces (octupole and octupole-octupole forces for negative-parity states) to the $P_0 + P_2 + QQ$ force.

References

[1] L.S. Kisslinger and R.A. Sorensen, Rev. Mod. Phys. 35 (1963) 853.

[2] M. Baranger and K. Kumar, Nucl. Phys. A 110 (1968) 529; 122 (1968) 241; 122 (1968) 273.

[3] T. Kishimoto and T. Tamura, Nucl. Phys. A 192 (1972) 246; 270 (1976) 317.

[4] A. Bohr and B. Mottelson, Nuclear Structure, vol. 2 (Benjamin, Reading,1975).

[5] K. Hara and S. Iwasaki, Nucl. Phys. A 348 (1980) 200.

[6] K. Hara and Y. Sun, Int. J. Mod. Phys. E 4 (1995) 637.

[7] T.T.S. Kuo and G.E. Brown, Nucl. Phys. A 114 (1968) 241.

[8] D.H. Gloeckner and F.J.D. Serduke, Nucl. Phys. A 220 (1974) 477.

[9] F.J.D. Serduke, P.D. Lawson and D.H. Gloeckner, Nucl. Phys. A 256 (1976) 45.

[10] R. Gross and A. Frenkel, Nucl. Phys. A 267 (1976) 85.

[11] A. Poves and A.P. Zuker, Phys. Rep. 70 (1981) 235.

[12] J. Blomquist and L. Rydstrom, Phys. Scr. 31 (1985) 31.

[13] X. Ji and B.H. Wildenthal, Phys. Rev. C 37 (1988) 1256.

[14] W.A. Richter, M.G. Van Der Merwe, R.E. Julies and B.A. Brown, Nucl. Phys. A 523 (1991) 325.

[15] J. Sinatkas, L.D. Skouras, D. Strottman and J.D. Vergados, J. Phys. G 18 (1992) 1377; 1401.

[16] E. Caurier, A.P. Zuker, A. Poves and G. Martínez-Pinezo, Phys. Rev. C 50 (1994) 225.

[17] W.A. Richter, M.G. Van Der Merwe and B.A. Brown, Nucl. Phys. A 586 (1995) 445.

[18] D. Rudolph, K.P. Lieb and H. Grawe, Nucl. Phys. A 597 (1996) 298.

[19] L. Zamick and M. Fayache, Phys. Rev. C 53 (1996) 188.

[20] H. Herndl and B.A. Brown, Nucl. Phys. A 627 (1997) 35.

[21] G. Martínez-Pinezo, A. Poves, L.M. Robledo, E. Caurier, F. Nowacki, J. Retamosa and A. Zuker, Phys. Rev. C 54 (1996) R2150.

[22] G. Martínez-Pinezo, A. Zuker, A. Poves and E. Caurier, Phys. Rev. C 55 (1997) 187.

[23] A. Poves and J.S. Solano, Phys. Rev. C 58 (1998) 179.

[24] K. Langanke, P. Vogel, Dao-Chen Zheng, Nucl. Phys. A 626 (1997) 735.

[25] K. Kaneko and Jing-ye Zhang, Phys. Rev. C 57 (1998) 1732.

[26] K. Kaneko, M. Hasegawa and Jing-ye Zhang, Phys. Rev. C 59 (1999) 740.

[27] M. Dufour and A. Zuker, Phys. Rev. C 54 (1996) 1641.

[28] K. Hara, Y. Sun and T. Mizusaki, Phys. Rev. Lett. 83 (1999) 1922.

[29] M. Hasegawa and K. Kaneko, Phys. Rev. C 59 (1999) 1449

[30] K. Kaneko and M. Hasegawa, Phys. Rev. C 60 (1999) 024301.

[31] K. Kaneko and M. Hasegawa, nucl-th/9907022 in the xxx.lanl.gov archive.

[32] E. Pasquini, Ph.D. thesis, Report No. CRN/PT 76-14, Strasburg, 1976.

[33] *Table of Isotopes*, 8th ed. by R.B. Firestone and V. S. Shirley (Wiley-Interscience New York, 1996).

[34] L. K. Peker, Nucl. Data Sheets 68 (1993) 271.

[35] J. A. Cameron *et al.*, Phys. Rev. C 58 (1998) 808.

[36] J. A. Cameron *et al.*, Phys. Rev. C 44 (1991) 1882.

[37] C. Frießner *et al.*, Phys. Rev. C 60 (1999) 011304.

[38] S. M. Lenzi *et al.*, Phys. Rev. C 60 (1999) 021303.

[39] F. Brandolini *et al.*, Nucl. Phys. A 642 (1998) 387.

[40] J. A. Cameron *et al.*, Phys. Rev. C 49 (1994) 1347.

[41] J. A. Cameron *et al.*, Phys. Lett. B 387 (1996) 266.

[42] T. W. Burrows, Nucl. Data Sheets 74 (1995).

[43] S. M. Lenzi *et al.*, Phys. Rev. C 56 (1997) 1313.

[44] T. W. Burrows, Nucl. Data Sheets 75 (1995).

[45] C. E. Svensson *et al.*, Phys. Rev. C 58 (1998) R2621.

[46] D. Rudolph *et al.*, Phys. Rev. Lett. 76 (1996) 376.

[47] D. J. Dean, S. E. Koonin, K. Langanke, and P. B. Radha, Phys. Lett. B 399 (1997) 1.

[48] F. Michel, G. Reidemeister and S. Ohkubo, Phys. Rev. C 34 (1986) 1248; Phys. Rev. Lett. 57 (1986) 1215; Phys. Rev. C 37 (1988) 292.

[49] S. Ohkubo *et al.*, Prog. Theor. Phys. Suppl. No. 132 (1998).

[50] M. Hasegawa and K. Kaneko, submitted to Phys. Rev. C, nucl-th/9907009 in the xxx.lanl.gov archive.

[51] J. Duflo and A.P. Zuker, Phys. Rev. C 59 (1999) R2347.

[52] M. Hasegawa and S. Tazaki, Nucl. Phys. A 633 (1998) 266.

[53] M. Hasegawa, Prog. Theor. Phys. Suppl. No. 132 (1998) 177.

[54] E. Caurier, J.L. Egido, G. Martínez-Pinezo, A. Poves, J. Retamosa, L.M. Robledo, and A. Zuker, Phys. Rev. Lett. 75 (1995) 2466.

[55] G. Martínez-Pinezo, A. Poves, L.M. Robledo, E. Caurier, F. M. Nowacki, J. Retamosa, and A. Zuker, Phys. Rev. C 54 (1996) R2150.

[56] J. Terasaki, R. Wyss and P.-H. Heenen, Phys. Lett. B 437 (1998) 1.

[57] T. Tanaka, K. Iwasawa and F. Sakata, Phys. Rev. C 58 (1999) 2765.